



Research Paper

Ce promoted V_2O_5 catalyst in oxidation of SO_2 reactionMohammad Mazidi^a, Reza Mosayebi Behbahani^{a,*}, Ali Fazeli^{b,c}^a Department of Gas and Chemical Engineering, Petroleum University of Technology (PUT), Ahvaz, Iran^b School of Chemical Engineering, College of Engineering, University of Tehran, Tehran, Iran^c Caspian Faculty of Engineering, College of Engineering, University of Tehran, Gilan, Iran

ARTICLE INFO

Article history:

Received 15 October 2016

Received in revised form

27 December 2016

Accepted 10 February 2017

Available online 14 February 2017

Keywords:

Catalytic performance

Ceria promoter

 SO_2 oxidation

Full factorial design

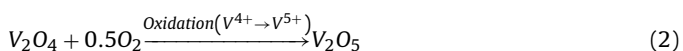
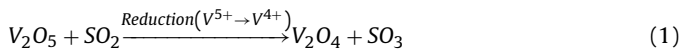
ABSTRACT

Harmful environmental effects of SO_2 on the start-up of the sulfuric acid plant process motivated studying ceria as a promoter for V_2O_5 catalyst that is employed in SO_2 oxidation. Effects of SO_2 (%), ceria percentage, temperature and O_2/SO_2 were investigated to optimize ceria loading on V_2O_5 catalyst. To determine the main and interaction effects, a full factorial design of experiments including 315 experiments was used. The results showed that the catalyst with 7 wt.% ceria (VaCe7) possessed the highest catalytic performance. To study the effect of more parameters on this catalyst, other 135 post-experiments with full factorial designs were performed after the optimization of Ce contents. The results revealed that mean SO_2 conversion increased with increasing SO_2 (%) and O_2/SO_2 ratio, and decreasing GHSV. Also, the maximum mean conversion was found at the reaction temperature of 450 °C by the trade-off of kinetic and thermodynamic factors of the reversible exothermic reaction. VaCe7 was found to have more catalyst activities than that the without-ceria (VaCe0) case. The synthesized catalysts were characterized by XPS, BET, FTIR, SEM, XRD and ICP. The SEM mapping revealed that the cerium oxide had better distribution on VaCe7 than VaCe9&11. FTIR, XRD and XPS showed the presence of $CeVO_4$ in the Ce-promoted catalyst and confirmed that ceria promotes V_2O_5 by the formation of $CeVO_4$ network, reduces the activation energy of reduction-oxidation and increases the rate of SO_2 oxidation reaction. The stability tests demonstrated good catalytic performance stability of the synthesized catalyst up to 50 h in the reaction. Results at the initial times of the stability tests showed that the catalyst with ceria promoter (VaCe7) had higher activity than VaCe0 at the start-up time. Also, VaCe7 had higher activity at the start-up than the its normal conditions, which could be related to the good oxygen storage capacity of ceria because the catalyst at the start up is faced to the oxygen of air. This high startup activity caused to use it in starting up of sulfuric acid plants that decreases SO_2 emission to the environment.

© 2017 Elsevier B.V. All rights reserved.

1. Introduction

Sulfuric acid is one of the most important chemical materials which can be produced by converting SO_2 into SO_3 over the supported liquid phase catalyst (V_2O_5 catalyst) that is used at 400–600 °C. Oxidation of SO_2 is performed on V_2O_5 catalyst according to the following Eqs. (1) and (2):



The reversible reaction of $V^{5+} \leftrightarrow V^{4+}$ is continually performed as a reduction-oxidation reaction [1]. Oxidation of sulfur dioxide to

trioxide plays an outstanding role in the sulfuric acid industry. SO_2 passes through V_2O_5 catalyst and takes up a large amount of SO_3 [2].

To prevent the release of SO_2 in the atmosphere, it is necessary to use a high-performance catalyst inside the reactor and decrease the catalyst degradation. Environmental atmospheric pollution (by SO_2 pollutant), water pollution (by dissolution of vanadium compound) and economic consideration (high consumption of V_2O_5 catalyst) encourage researchers to synthesize the high-performance V_2O_5 catalyst [3–5]. One of the most important ways is to add promoters such as Rb, Cs, rare earth metals, lanthanide metals and alkali metals to increase the efficiency of the process. Industrial catalysts have been studied for modification by these promoters [6,7].

So far, various efforts have been made to develop the properties of V_2O_5 catalyst, e.g. adding Rb and Cs [6]. However, ceria as a promoter has been never used over vanadium catalyst in SO_2 oxidation. Ceria as a metal oxide has the ability to store or release

* Corresponding author.

E-mail address: Behbahani@put.ac.ir (R. Mosayebi Behbahani).

oxygen between Ce^{4+} and Ce^{3+} [8]. Some researchers have studied the effect of Rb, Cs and Rb-Cs promoters on V_2O_5 catalyst. CS-Rb-V catalyst has shown higher catalytic activities at low temperature [6]. Low temperature, in turn, has some advantages such as decreasing the capital investment and operating cost as well as shortening the start-up time [1]. Promoters such as rare earth, alkali and lanthanide metals can be used in V_2O_5 catalyst to increase activity. However, cesium promoter has much higher performance than Rb and Li [9–14]. Rare earth oxides have been used in some catalyst applications and CeO_2 is well-known as a light rare earth element [15]. CeO_2 has unique physiochemical properties such as stability, selectivity and activity in some catalytic applications. Researchers have used the oxygen-storage capacity of CeO_2 in their publications such as the effect of CeO_2 on Ni catalyst to increase the activity and reduce the coke formation [16]. The oxygen storage capacity can be defined as a local source to store or release oxygen [17]. A few researchers have investigated vanadium and cerium interaction, which has no application in SO_2 oxidation process [18–20]. Information about the interface of vanadium-cerium has been studied for the oxidative hydrogenation of hydrocarbons [21] and is undetermined for SO_2 oxidation reaction.

The unique role of cerium in the reversible redox reaction of $\text{Ce}^{3+} \rightleftharpoons \text{Ce}^{4+}$ has been investigated. During this reaction, oxygen is released and reacts with other reactants. Also, oxygen storage capacity makes it suitable for use in the oxidation of CO to CO_2 [22,23]. Reduction of Ce^{4+} to Ce^{3+} and concentration of Ce^{3+} ion in this reaction are related to oxygen vacancy [24]. Enhancing the migration of lattice oxygen in CeO_2 catalyst is a unique property to encourage researchers to use this material in their studies [25–28]. Besides, CeO_2 has some advantages such as local source or sink for oxygen vacancy that can be useful for the surface of catalyst [29]. Cerium has been used in water gas shift reaction [30], catalysts in automobile exhaust [31] and wet oxidation of acrylic acid [32]. In automotive exhaust catalysis, the excess of oxygen is adsorbed on the reduced ceria and, when there is insufficient oxygen in the stream, ceria releases oxygen [33]. An outstanding property of ceria is the release and up-taking of lattice oxygen in the chemical reaction [34]. Recently, some researchers studied the role of Ce as a promoter such as Yang et al. [35] that describes the role of Ce promoter in enhancing Ni/SBA-15 catalyst activity for anisol hydrotreating. Mendes et al. [36] reported that adding low concentration of CeO_2 to the Pd-MOR catalysts increases the catalyst activity in the selective reduction of NO_x . Pizarro et al. [37] studied the effect of adding Ce to pillared clay-supported Pt and Ir catalysts for aqueous-phase hydrodechlorination and report that the synergistic effect of Ce and Pt was not repeated in Ir catalyst. Arena et al. [38] have a research on the positive role of Ce on structure and reactivity of MnO_x catalysts in the liquid phase selective oxidation of benzyl alcohol. But the role of Ce promoter on V_2O_5 catalyst was never studied in SO_2 oxidation and before this research, it cannot be predicted that Ce have a positive or negative effect on this catalyst performance.

Reducing SO_2 emission is a widespread interest in the sulfuric acid plant. SO_2 is one of the six gases that pollutes air according to 1970 Clean Air Act [39]. Sulfur dioxide is produced in sulfur burning plants in a furnace and the ratio of sulfur to air is adjusted within desirable limits. The produced SO_2 and unconverted oxygen react to produce SO_3 in a convertor containing 4–5 beds. Lack of oxygen in the furnace can reduce the oxidizing of SO_2 to SO_3 in the convertor and lead to the high concentration of SO_2 in the exhaust gases of the stack, which are dangerous for humans and the environment. This ratio is constant for normal operation, but it fluctuates at the start-up of the plant, which causes the release of a large part of SO_2 gases to the atmosphere. Also, the catalytic activity at start up of plant is low, because of low temperature of the catalyst bed at

Table 1
Full factorial design for detecting the best percentage of ceria in V_2O_5 catalyst.

Notations	Variables	Number of levels	Levels
SO_2	Percentage of SO_2 (%)	3	6–9–12
O_2/SO_2	Percentage of O_2 to SO_2	3	0.8–1–1.2
Temp	Temperature($^{\circ}\text{C}$)	5	410–450–490–530–570
Ce	Percentage of Ceria (%)	7	0–1–3–5–7–9–11

starting up. SO_2 emission forms acid rain that can be a dangerous environmental problem [40]. Using catalyst with higher activity can reduce the SO_2 emission. This emission has a bad effect on the respiratory system. However, the start-up of sulfuric acid plants has received less attention in view point of catalyst. The environmental concern of this problem has led to the use of high-performance catalyst to overcome it. As a result, the catalyst must work properly with higher activity at starting up than normal operating temperature and it should convert SO_2 to SO_3 in the reactor normally in this start-up condition.

In this article, ceria was studied as a promoter of V_2O_5 catalyst to find whether this promoter had the synergistic effect on vanadia and any role in improving the SO_2 oxidation catalyst activity. Also, the amount of ceria promoter was optimized in this study by an experimental design. Effects of $\text{SO}_2\%$, O_2/SO_2 ratio, temperature, GHSV and their interactions on the optimized ceria-promoted catalyst were investigated. Catalysts were characterized by XPS, FTIR, BET, XRD, ICP and SEM methods and the role of ceria promoter on the catalyst performance was justified by the characterization results.

2. Experimental

2.1. Catalyst preparation

Ceria-promoted V_2O_5 catalyst was prepared with various concentrations of ceria according to the procedure shown in Fig. 1. Potassium hydroxide was mixed with deionized water and then mixed with glass water ($\text{SiO}_2/\text{Na}_2\text{O} = 2.61$), V_2O_5 , H_2SO_4 and diatomaceous earth (Mianeh Mine treated with 15 wt.% sulfuric acid) according to Fig. 1 [41]. Cerium nitrate hexahydrate was dissolved in deionized water and impregnated in the paste. The paste was dried at 110°C for 5 h and calcinated at 550°C for 3 h.

2.2. Material

Cerium (III) nitrate hexahydrate, sulfuric acid with the purity of 99.99%, V_2O_5 , water glass and chemical materials for iodometry were supplied by Aldrich Chemical Company. Mianeh (Mi) diatomite treated with 15 wt.% sulfuric acid, was used as a catalyst support [41]. SO_2 (99.98%), O_2 (99.998%) and N_2 (99.999%) gases were purchased from Roham Gas Company.

2.3. Method

Firstly, the experiments were performed at different levels with various variables which are listed in Table 1. The experiments were designed at three levels of SO_2 , three levels of O_2/SO_2 , five levels of temperature and seven levels of CeO_2 percentage in the catalyst (Gas Hourly Space Velocity = 6000 h^{-1}). The full factorial method was applied for the design of the experiments to study the interaction between all the variables. Finally, $3^*3^*5^*7 = 315$ experiments were performed to select the best percentage of cerium oxide on V_2O_5 catalyst.

After finding the best percentage of ceria on V_2O_5 catalyst, some experiments were performed with the change of four factors (Per-

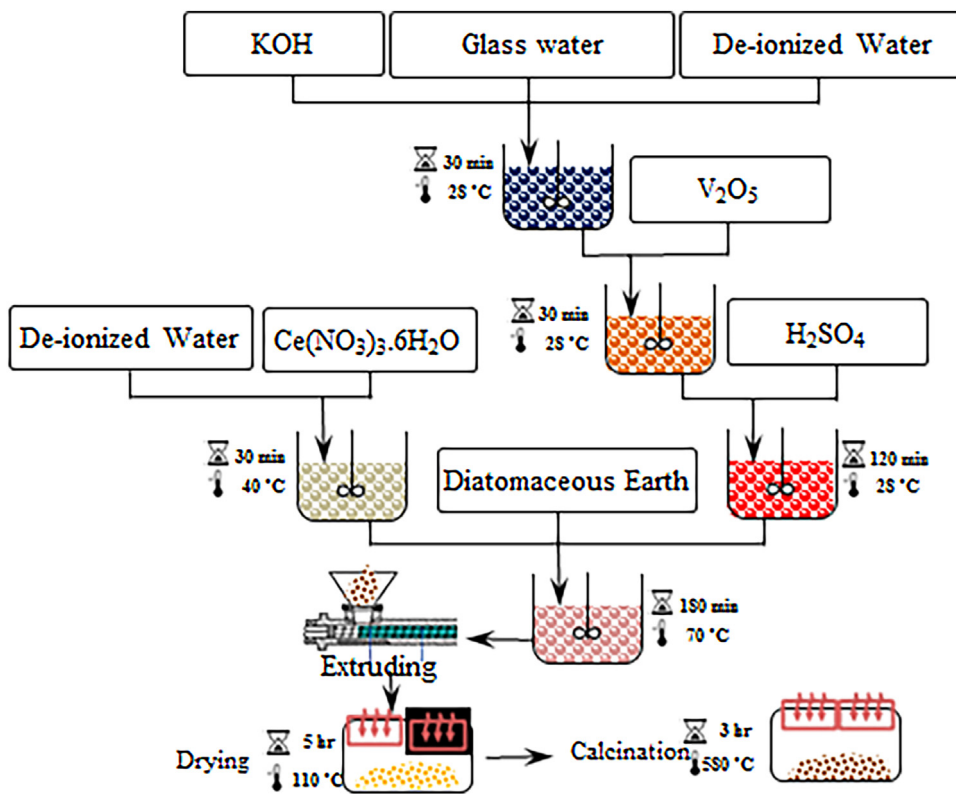


Fig. 1. Synthesis procedure of ceria promoter V_2O_5 catalyst.

Table 2

Full factorial design for studying interaction between variables.

Notations	Variables	Number of levels	Levels
SO_2	Percentage of SO_2 (%)	3	6-9-12
O_2/SO_2	O_2 to SO_2	3	0.8-1-1.2
Temp	Temperature (°C)	5	410-450-490-530-570
GHSV	Gas Hourly Space Velocity (hr ⁻¹)	3	6000-15000-30000
Ce	Percentage of ceria (%)	2	0-7

centage of SO_2 , O_2 to SO_2 , GHSV and Temperature) in the full factorial design. These experiments consisted of $3^*3^*3^*5 = 135$ trials for each catalyst with Ce (VaCe7) and without Ce (VaCe0) to study the preference of the catalyst with the best ceria promoter percentage (VaCe7) to the reference catalyst (VaCe0) by considering various variables listed in Table 2 and their interactions. Table 2 shows the variables and levels of these experiments. The response variable in this study was SO_2 conversion and, for the analysis of the results, the main effect plot of the response was illustrated as a function of the variables. In this plot, the mean of the response (mean conversion) was used for each level of the variables.

2.4. Characterization

To study the structure and crystallinity of the samples, X-ray powder diffraction (XRD) was performed by a Bruker AXS D8 advanced diffractometer using Cu K α radiation. To determine the percentage of V_2O_5 and CeO_2 , ICP (inductively coupled plasma) test was carried out by ICP Elementary Analyzer (PerkinElmer[®] OptimaTM 8000). IR spectra were used to detect the functional groups of the various catalysts with recording on Bomemmb-series 1998 FT-IR spectrometer. Surface morphology of the catalyst was investigated by scanning electron microscopy (SEM) (Vega Ts

5136MM, Tescan Company) instrument. N_2 adsorption/desorption was also used to study the BET surface area and pore characterization of various catalysts. An automated gas adsorption analyzer (Tristar 3020, Micromeritics) was used for BET tests. X-ray photo-electron spectroscopy (XPS) spectra of the catalyst were performed by a scanning X-ray microprobe (AXIS Ultra) equipped with a monochromatic Al K α radiation (1486.6 eV). All of the binding energies were obtained by C 1S line (BEs = 284.8 eV) as the standard.

2.5. Catalyst pretreatment and performance

To evaluate the performance of the synthesized catalysts, catalyst activity test was carried out in a fixed bed quartz tube reactor according to Fig. 2. Three MFCs (mass flow controllers/Brooks) were used for SO_2 , O_2 and N_2 gases. The catalyst powders with the mesh size of 40–60 were charged into the reactor

To monitor the temperature of the catalyst, a thermocouple (Omega K-type) was used at the bottom of the catalyst bed. These catalysts were pretreated by passing the feed over them from ambient to reaction temperature and maintain the feed passing the catalyst for 150 min to reach a stable activity. After 150 min passing the feed, the status of catalyst active sites reaches to a stable condition and activity line goes ahead horizontally by increasing the time. But for more precision, all the reported activity were measured after 500 min. Catalyst performance was tested at 410–570 °C in the steps of 40 °C SO_2 concentrations in the feed and reactor outlet were measured by iodometry method [42].

SO_2 Conversion is defined as the following Eq. (3):

$$X_{SO_2}(\text{Conversion}) = \frac{n_{SO_2}^{in} - n_{SO_2}^{out}}{n_{SO_2}^{in}} \times 100 \quad (3)$$

where

$n_{SO_2}^{in}$ is inlet molar flow rate of SO_2

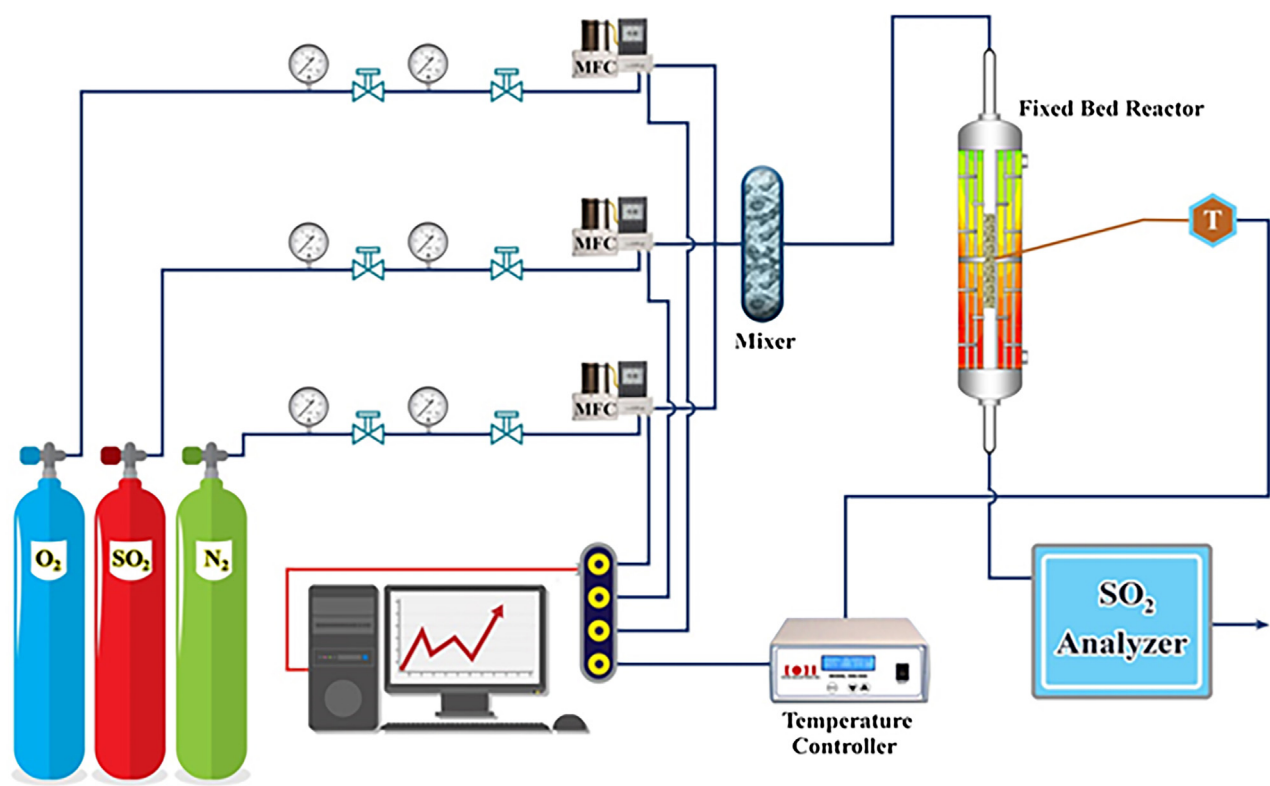


Fig. 2. Scheme of conversion test for V_2O_5 catalyst.

$n_{SO_2}^{out}$ is outlet molar flow rate of SO_2

3. Results and discussion

3.1. N_2 adsorption/desorption analysis

The structural properties of various samples with different percentage of ceria promoter are listed in Table 3. In this table, vanadia loading, ceria loading, BET surface area and average pore size are tabulated. All the codes of the synthesized catalyst with various levels of ceria promoter (wt.%) were nominated as $VaCe_{cerialoading\%}V_2O_5$ catalyst without ceria promoter ($VaCe0$) showed high BET and average pore size, which were $3.8\text{ m}^2\text{gr}^{-1}$ and 61 nm, respectively. It can be observed that with increasing the cerium content on V_2O_5 catalyst from 0 to 11%, BET surface areas and average pore size were decreased gradually. It can be attributed to the migration of ceria promoter to the pores of the catalyst and clogging some pores by the addition of ceria promoter to V_2O_5 catalyst.

Pore size distribution and N_2 adsorption/desorption can be seen in Fig. 3a-b. As observed, pore size distribution (PSD) is shown at the range of the mesopores and macropores between 5–190 nm that it was decreased with increasing the ceria pro-

moter. In addition, PSD of $VaCe0$ was greater than that of other samples and PSDs were changed in the following sequence of $VaCe0 > VaCe1 > VaCe3 > VaCe5 > VaCe7 > VaCe9 > VaCe11$. Enhancing ceria loadings shifted PSD to less pore size, which might be attributed to the movement of ceria promoter to the pores and reduction of PSD. The samples ($VaCe9$ and $VaCe11$) with higher content of ceria showed a broad PSD. Finally, ceria promoter decreased the PSD of the catalyst. The N_2 adsorption/desorption can be observed in Fig. 3b. The result indicated the similar profiles for $VaCe0$ to $VaCe11$. The N_2 adsorption/desorption revealed a type of IV isotherm with a large H3-type hysteresis loop at about $P/P_0 = 0.35–0.98$ according to the IUPAC classification. This hysteresis loops suggested the agglomerates of the particles with slit-shaped pores and non-uniform size (like cubes). This result had an excellent agreement with the SEM result in the inset picture of Fig. 3b. Higher relative pressure (P/P_0) was proportional to the large mesopores in the catalyst [43].

3.2. Effect of ceria promoter

The results of the experiments tabulated in Table 1 with full factorial design are illustrated in Fig. 4a-c. Fig. 4a displays the effect of ceria promoter on SO_2 conversion of V_2O_5 catalyst at various temperatures of 410–570 °C. The results demonstrated the

Table 3
Structural properties of sample with various percentages of ceria promoters on V_2O_5 catalyst.

No.	Sample	Nominal Composition	Vanadia Loading (Wt.%)	Ceria Loading (Wt.%)	$S_{BET}(\text{m}^2/\text{gr})$	Average Pore size (nm)
1	$VaCe0$	Va/SiO_2	7	0	3.8	61
2	$VaCe1$	$Va/Ce/SiO_2$	7	1	3.4	56
3	$VaCe3$	$Va/Ce/SiO_2$	7	3	3.1	55
4	$VaCe5$	$Va/Ce/SiO_2$	7	5	3	48
5	$VaCe7$	$Va/Ce/SiO_2$	7	7	2.7	44
6	$VaCe9$	$Va/Ce/SiO_2$	7	9	2.3	36
7	$VaCe11$	$Va/Ce/SiO_2$	7	11	2	33

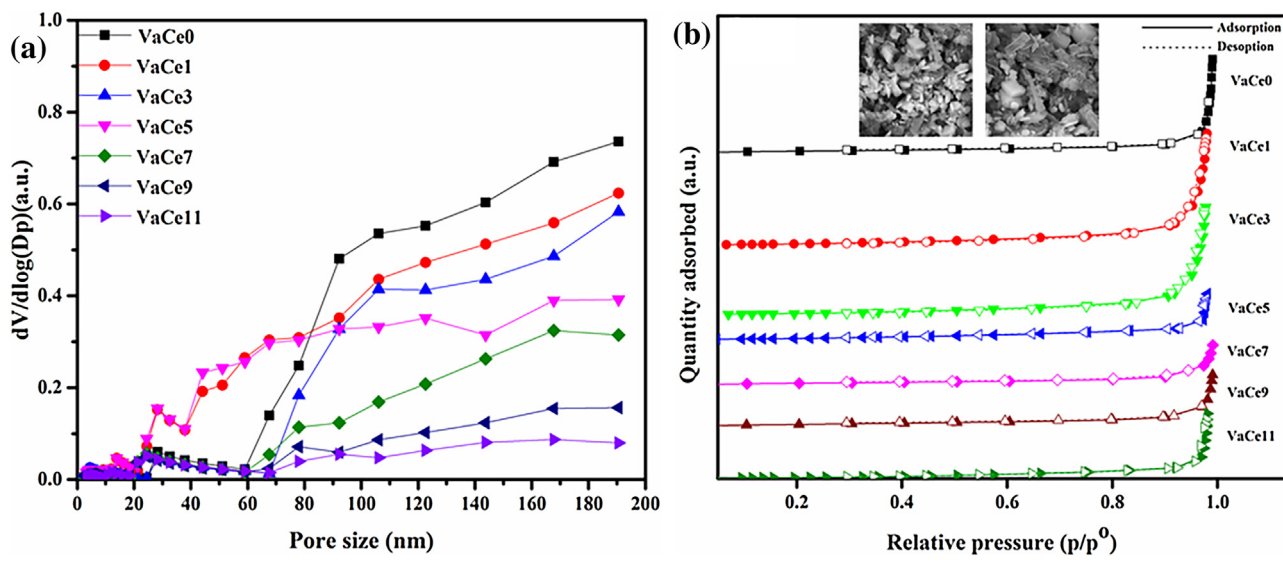


Fig. 3. (a) Effect of ceria promoter on pore size distribution of samples, (b) Effect of ceria promoter on N₂ adsorption/desorption profiles.

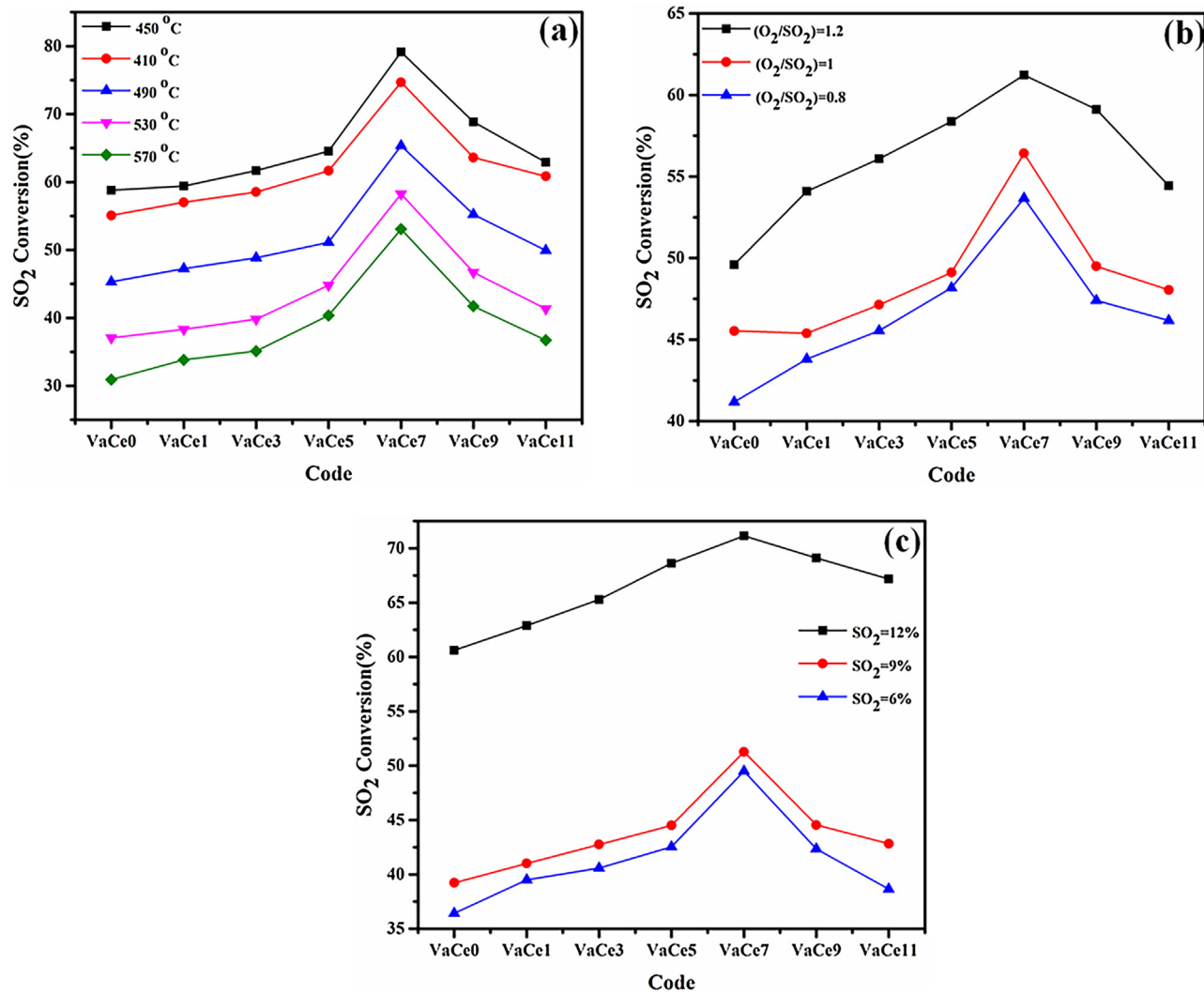


Fig. 4. Effect of ceria promoter concentration on SO₂ conversion at various (a) temperature from 410 to 570 °C, (b) O₂/SO₂ ratio from 0.8 to 1.2% and (c) SO₂% at feed from 6 to 12%.

significant effect of ceria loading on the catalytic activity. It was obvious that with enhancing the ceria content on the catalyst, the SO_2 conversion was increased. This conversion slightly increased from 59 to 79% at 450 °C with increasing the ceria loading from 0 up to 7 wt.%, respectively, but SO_2 conversion was reduced at the higher percentage of ceria content in the catalyst. Briefly, the trends of SO_2 conversion versus ceria promoter content at other temperatures (410, 490, 530 and 570 °C) was similar to the curve at 450 °C. According to Fig. 4a, the conversion of SO_2 rose from 410 to 450 °C and reduced from 450 to 570 °C because of the reaction exothermicity and thermodynamic equilibrium limitation. The results demonstrated that rising the ceria promoter from 0 to 7 wt.% increased SO_2 conversion at least 35% because ceria has oxygen vacancies in its structural network that plays an important role in oxygen transfer [44]. With more increasing (after 7 wt.%) in ceria content, the activity decreased due to the low dispersion of ceria promoter on the catalyst, which will be discussed in SEM observation.

Fig. 4b shows SO_2 conversion versus ceria promoter content at various O_2/SO_2 ratios. As can be seen, SO_2 conversion was enhanced dramatically by increasing ceria promoter from 0 to 7 wt.% ceria loading and, then, decreased from 7 to 11 wt.% ceria loading for $\text{O}_2/\text{SO}_2 = 0.8$ and 1. In addition, conversion increased gradually by rising ceria promoter to 7 wt.% and, then, dropped to 11 wt.% for $\text{O}_2/\text{SO}_2 = 1.2$. Therefore, Fig. 4b, shows that the SO_2 conversion was

elevated by O_2/SO_2 ratio in the range of $\text{O}_2/\text{SO}_2 = 0.8–1.2$ and higher catalytic activity can be seen at the higher ratio of O_2/SO_2 in the range of experiments. It may be deduced that oxygen vacancies can be enriched at higher O_2/SO_2 . Also, the slopes of the curves at $\text{O}_2/\text{SO}_2 = 0.8$ and 1 were higher than $\text{O}_2/\text{SO}_2 = 1.2$, suggesting that the sensibility of SO_2 conversion into ceria content at lower O_2/SO_2 was more than the higher ratio. Although with increasing the ceria loading, the BET surface area was decreased (caused a decrease in the contact time between reactants and active phase), the catalytic activities were increased with increasing the ceria loading up to 7%. According to the literature, cerium oxide network had oxygen vacancies [45,46]. It may be concluded that the positive role of oxygen vacancy in adding CeO_2 to the catalyst overcame the negative effect of decreasing the BET surface area.

Finally, the obtained results revealed that V_2O_5 catalyst with 7 wt.% of ceria content had the highest activity among other synthesized catalysts. Indeed, SO_2 conversion was elevated by O_2/SO_2 ratio. Large oxygen storage capacity (OSC) of ceria can make more oxygen available for the oxidation reaction [47,48]. As may be deduced, oxygen storage capacity (OSC) of CeO_2 was increased at higher O_2/SO_2 ratio.

Effects of SO_2 concentration on the activity performance of catalyst are illustrated in Fig. 4c. This figure shows that increasing the feed SO_2 concentration increased the catalyst activity at all ceria promoter contents. Also, the results demonstrated that the addi-

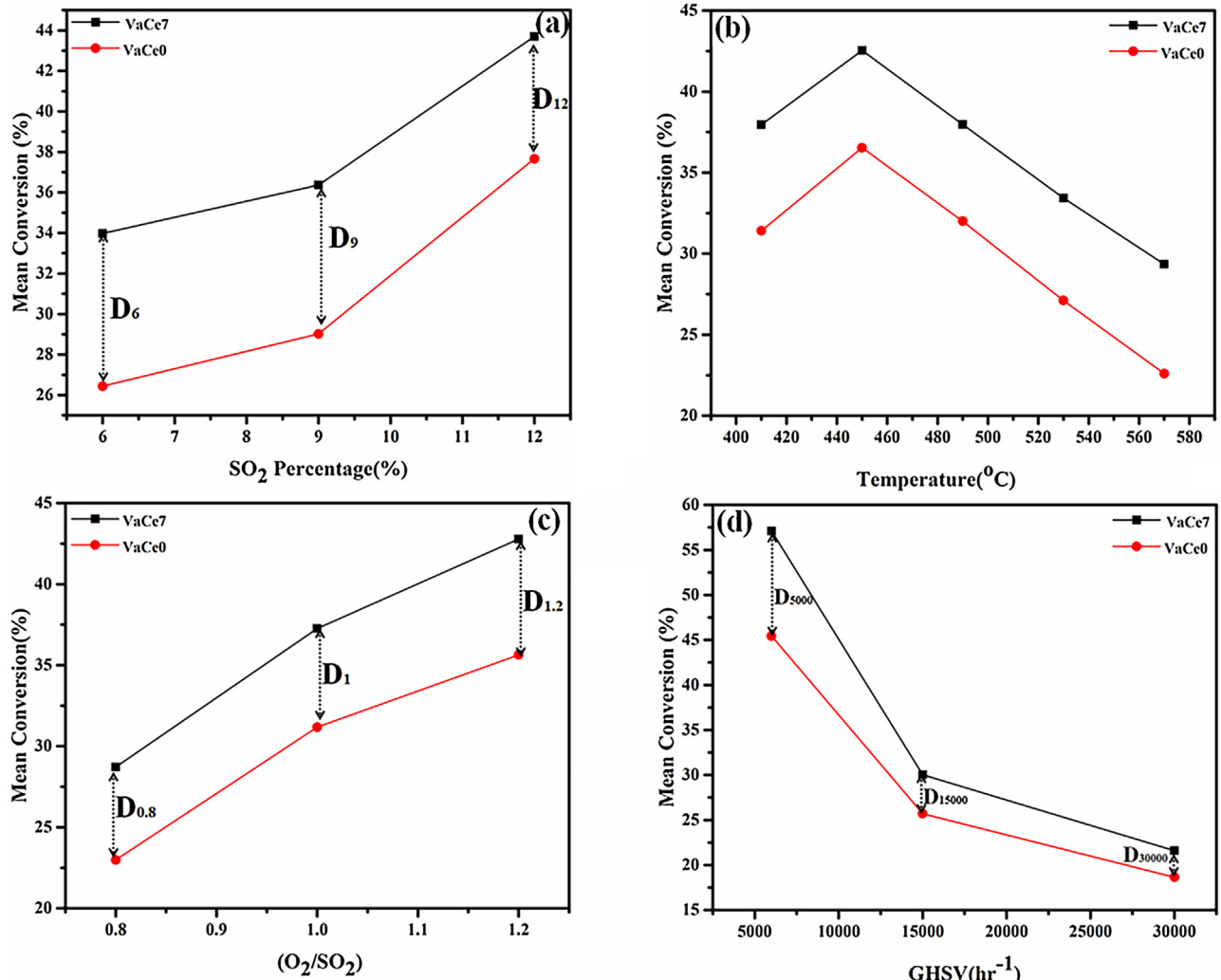


Fig. 5. Effect of mean SO_2 conversion at VaCe0 and VaCe7 samples on (a) feed $\text{SO}_2\%$, (b) temperature, (c) O_2/SO_2 ratio and (d) Gas hourly space velocity.

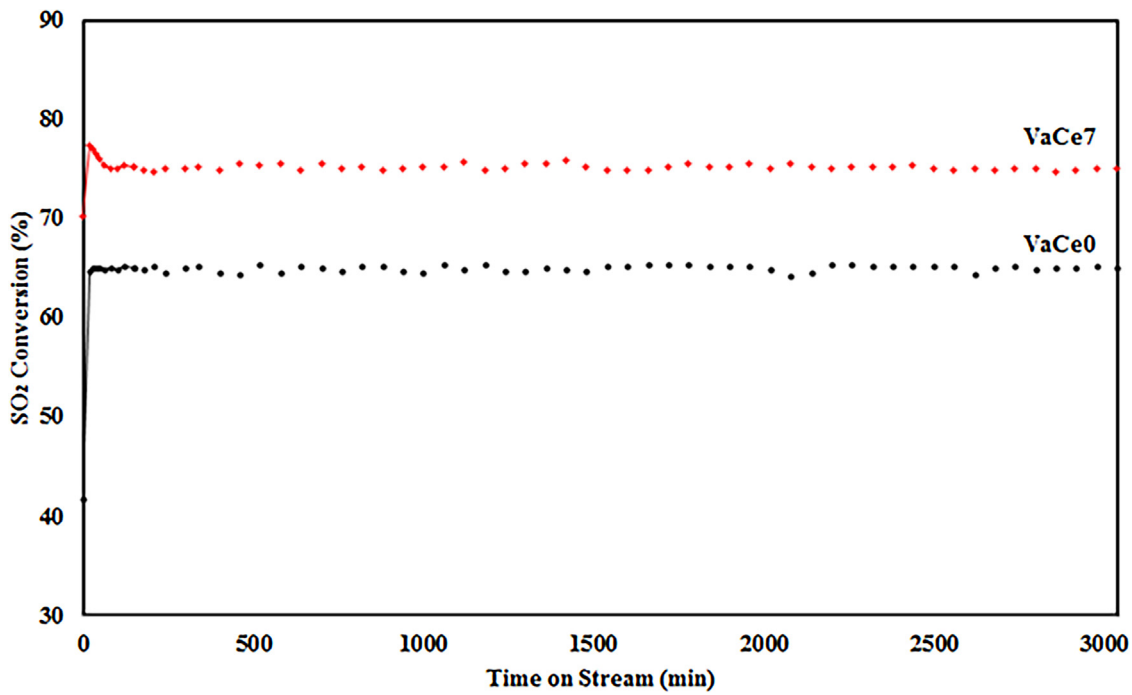


Fig. 6. Stability of VaCe0 and VaCe7 at (GHSV = 6000 h⁻¹, temperature = 450 °C, SO₂ = 12% and O₂/SO₂ = 0.8).

tion of ceria promoter improved the SO₂ conversion up to 7 wt.% CeO₂ sharply and reduced the conversion from 7 to 11 wt.% ceria content in the case of 6 and 9% SO₂. In contrast to these sharp curves, in the case of 12% SO₂ in the feed, rising this curve up to 7 wt.% and dropping it from 7 to 11 wt.% is gradual.

Fig. 4(a–c) represents the relationship of SO₂ conversion and ceria loading on V₂O₅ catalyst that was volcano-shape. The highest activity of the catalyst can be observed with 7 wt.% ceria promoter (VaCe7) on V₂O₅ catalyst, which might be related to the excellent dispersion of ceria on the catalyst. Consequently, the oxygen vacancy on the surface of the catalyst was a valuable parameter for the reaction of the available oxygen with SO₂ [49]. As the result of the fact that oxygen storage capacity can be provided with the reduction and re-oxidation of ceria [33], the positive behavior of ceria may affect SO₂ reaction. All the experiments of Table 1 showed an optimum ceria loading in this reaction that was 7 wt% ceria content. Therefore, this sample (VaCe7) was selected for more investigation in this research. The effect of operating condition will be studied in this optimum sample (VaCe7) according to Table 2 for the design of the experiments.

3.2.1. Preference of VaCe7 to VaCe0

As presented in Table 2, various parameters were selected to study the main effect and their interactions. The results of all the parameters are shown in Fig. 5a–d. The interaction of GHSV with other variables was also studied, which has been rarely focused in the study of SO₂ oxidation reaction.

Fig. 5a is the main effect plot of SO₂% on conversion percentage in two cases of VaCe7 and VaCe0. The two curves were ascending, which showed that increasing SO₂%, increased the conversion. It can be observed that VaCe7 curve was always on top of VaCe0. The difference of the mean conversion of VaCe7 and VaCe0 at various levels of SO₂% were nominated D_{SO2%}. The results showed that D₆ > D₉ > D₁₂ and this observation proved that VaCe7 had higher mean conversion difference at lower SO₂%. It can be concluded that adding 7%Ce at lean SO₂ feed had more effects than VaCe0.

Fig. 5b shows the effect of temperature on mean conversion (%) in two samples (VaCe0 and VaCe7). VaCe7 had more mean conver-

sion than VaCe0 at all temperatures. These two curves showed the maximum mean conversion at 450 °C due to the trade-off kinetic and thermodynamic in this reversible exothermic reaction.

Fig. 5c displays that effect of O₂ to SO₂ ratio on the mean conversion for two samples: VaCe0 and VaCe7. Two samples showed the ascending trend with raising the ratio of O₂ to SO₂. The curves of VaCe7 were always higher than VaCe0 curves. The difference of the mean conversions of VaCe7 and VaCe0 at various levels of O₂/SO₂ ratio was nominated D_{O2/SO2}. Mean SO₂ conversions (%) in this figure followed the sequence D_{1.2} > D₁ > D_{0.8}. These results demonstrated that VaCe7 had higher mean conversion difference at higher O₂/SO₂ ratio compared with the lower O₂/SO₂ ratio.

Fig. 5d represents the effect of Gas Hourly Space Velocity (GHSV) on mean SO₂ conversion in two samples (VaCe0 and VaCe7). Two curves were descending, showing that raising GHSV decreased the mean SO₂ conversion. Also, VaCe7 curve was on top of VaCe0 curve. The difference of mean SO₂ conversion of VaCe7 and VaCe0 at various levels of GHSV was designated D_{GHSV}. The result showed the following sequence of D₆₀₀₀ > D₁₅₀₀₀ > D₃₀₀₀₀. It can be deduced that mean SO₂ conversion decreased with increasing GHSV due to reducing the contact time between the reactants and catalyst active sites.

The main effect plots of Fig. 5a to d indicated that O₂ to SO₂ ratio and concentration of SO₂ reactant had a favorable effect and GHSV had an inverse effect on mean SO₂ conversion percentage.

3.2.2. Stability test

Fig. 6 presents SO₂ conversion versus time on stream (TOS), which showed the long-term stability of the synthesized catalyst (VaCe0 and VaCe7) with various ceria contents at 450 °C. Two prepared catalysts (VaCe0 and VaCe7) demonstrated high long-term stability without any decrease (deactivation) in SO₂ conversion that was tested during 3040 min of the oxidation reaction. At the start-up time, the catalyst activity increased rapidly and, after about 150 min, it reached the stable line, which may be related to the preparation of the catalyst active sites. Based on the stability experiments, the activity of the catalyst in all the experiments must be recorded after 150 min, but for more confidence, all the activity data

were gathered after 500 min. The activity of VaCe0 in this period of the experiment (3040 min ~ 50 hr) fluctuated around the average of 65% and also the average conversion of VaCe7 was around 75%. It can be deduced that adding ceria promoter with 7 wt.% to V_2O_5 catalyst could highly improve the performance of SO_2 oxidation reaction. Therefore, to decrease SO_2 emission in industrial applications, a sufficient amount of rare earth could be added to V_2O_5 catalyst, which could cause more activity and that remains stable.

Studying Fig. 6 at the start-up times showed that the conversion on the catalysts VaCe7 and VaCe0 was 70 and 40%, respectively, which was 93% and 62% of the stable conversions. This issue demonstrated that ceria could promote the conversion by storing oxygen and transferring it to V_2O_5 . Also, the peak of the conversion at the start-up time went above the stable conversion for VaCe7 catalyst and this peak did not exist at the start-up of VaCe0 catalyst. This phenomenon is important for reducing SO_2 emission at starting-up the sulfuric acid plant. Adsorbed oxygen on ceria as a promoter could increase the conversion at this time and reduce the environmental problems of starting-up of these plants.

3.3. FTIR spectra

The FTIR spectra of V_2O_5 catalyst without (VaCe0) and with (VaCe7) ceria promoter are shown in Fig. 7. Considerable adsorbed H_2O on the surface of VaCe0 and VaCe7 can be detected in 1630 cm^{-1} band [50]. The bands between 1000 and 1200 cm^{-1} represents that the sulfur species are adsorbed on the surface of catalyst [51]. In VaCe0 sample, some peaks were observed at 1040, 994, 935 and 1050 cm^{-1} that can be assigned to the surface species of SO_2 , bulk V_2O_5 species, split v_3 stretching vibrating of SO_3^{2-} and v_3 of SO_4^{2-} groups in $S_2O_7^{2-}$, respectively [52–55]. In VaCe7 sample, it can be concluded that the peak at 996 was attributed to CeO_2 [56]. In two samples of VaCe0 and VaCe7, we can observe some peaks at 800, 600–700, 592, 611–615 cm^{-1} and 960–980, which can be attributed to asymmetric SOS stretching, indicating $S_2O_7^{2-}$, v_4 vibration of SO_4^{2-} group, vanadyl sulfoxide species, $VO(SO_4)_2$ and sulfate samples, respectively [57,58]. In VaCe7 catalyst, the shoulder of peak in 800 cm^{-1} that was located at 737 cm^{-1} is for the VO_4 units in the shape of orthovanadate and intense peak in 800 cm^{-1} for VaCe7 sample shows the $CeVO_4$ component [59,60]. As a matter of fact, a strong absorption band at 800 cm^{-1} and a weak band at 520 cm^{-1} may be assigned to the absorption of $V-O$ and $Ce-O$ bands, respectively. Eventually, these bands demonstrate the production of $CeVO_4$ in this catalyst [61,62].

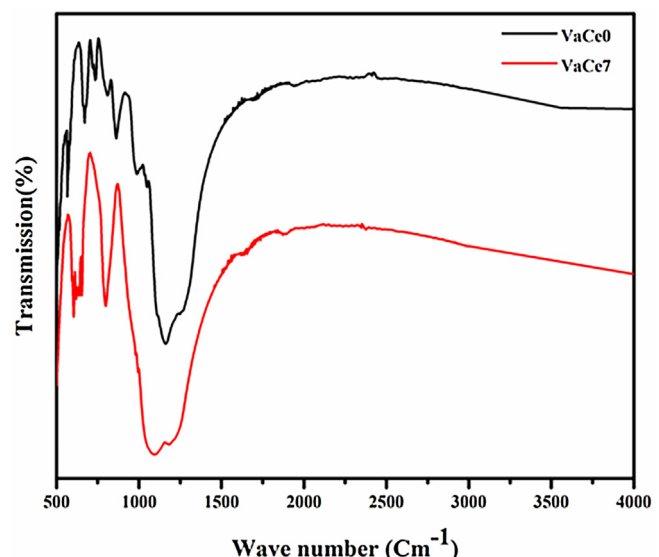


Fig. 7. FTIR spectra of VaCe0 and VaCe7 samples.

3.4. X-ray diffraction

The XRD patterns of VaCe0 and VaCe7 samples, without and with ceria promoter, are shown in Fig. 8. VaCe7 sample showed the diffraction peaks at 21.7 , 28.5 and 29.7° , which corresponded to $[001]$, $[200]$ and $[111]$ planes for vanadyl sulfate (code 00-024-1394), diffraction peaks at 9.1 , 13.84 , 21.69 , 24.97 , 29.7 , 33.5 and 35.49° , which corresponded to $[001]$, $[110]$, $[211]$, $[121]$, $[013]$, $[113]$ and $[032]$ planes for vanadium oxide sulfate (code 01-076-2154), and diffraction peaks at 11.64 , 21.69 , 28.38 , 29.71 and 33.50° for potassium cerium sulfate (code 00-39-0646), diffraction peaks at 16.3 , 20.4 , 24.7 , 26.4 , 28 and 55.95° , corresponding to $[-101]$, $[-111]$, $[020]$, $[200]$, $[120]$ and $[-412]$ planes for cerium vanadium oxide ($CeVO_4$ with code 00-023-0150), diffractions peaks at 28.5 , 33 and 56.3° which corresponded to $[111]$, $[200]$ and $[311]$ for cerium oxide (CeO_2 with code 00-034-0394) and diffraction peaks at 21.8 , 38.6 and 44.6° for cristobalite low (code 01-076-0940).

VaCe0 sample showed the diffraction peaks at 21.86 , 26.52 , 27.18 and 30.7° for potassium vanadium oxide sulfate (code 00-033-1056), diffraction peaks at 21.8 , 31.8 and 44.5° for potassium

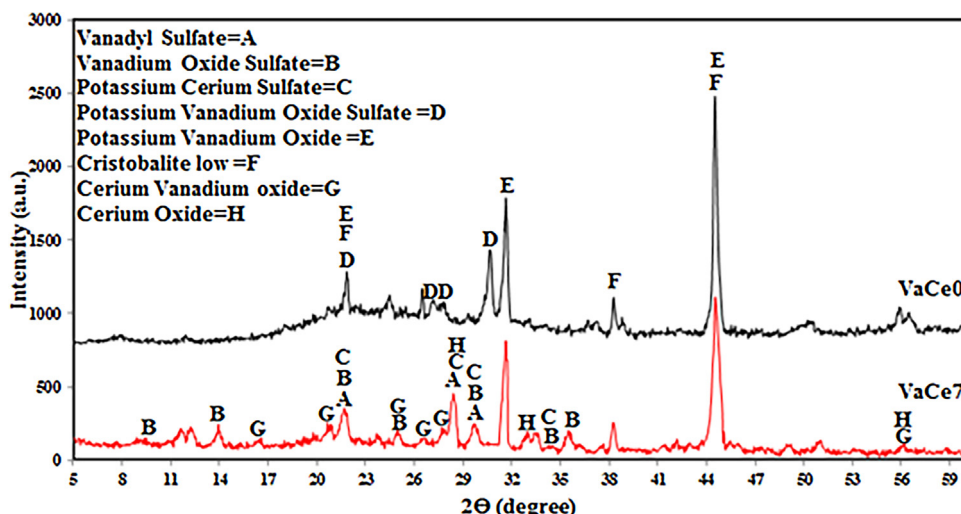


Fig. 8. XRD pattern of VaCe7 and VaCe0 samples.

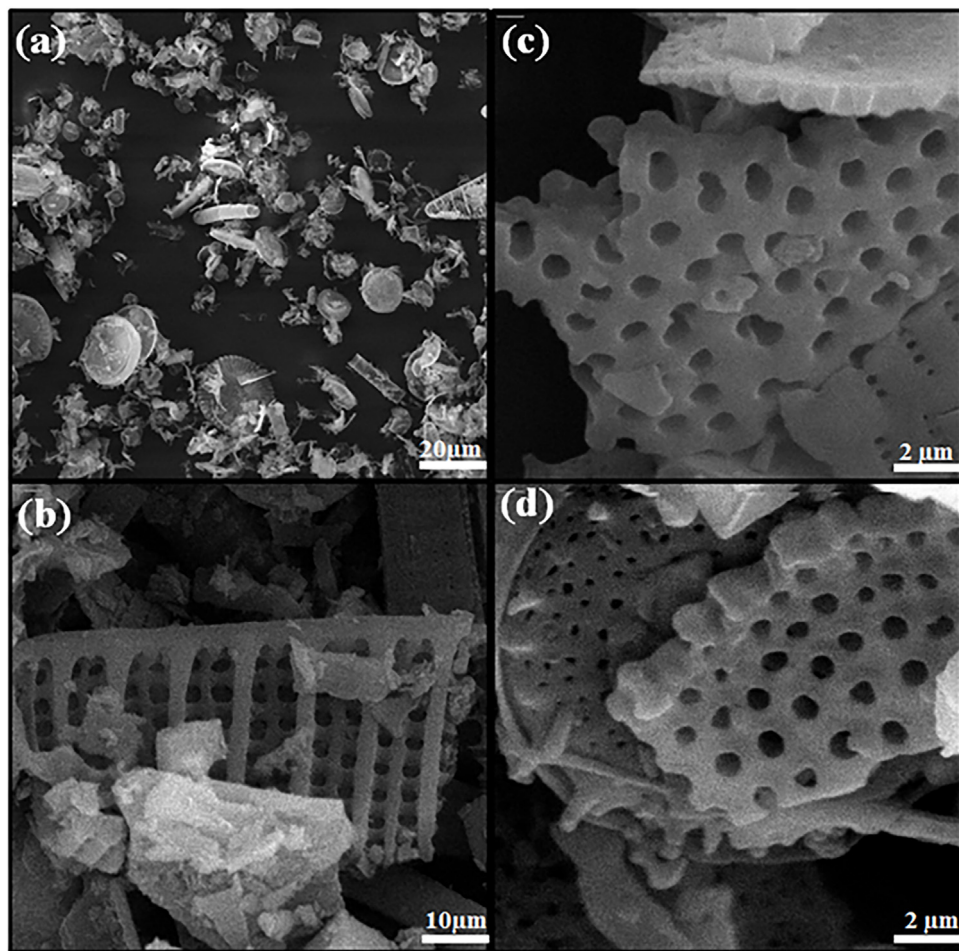


Fig. 9. SEM images of diatomaceous earth as catalyst support (a) Various shapes of diatomite, (b) cylindrical shape of diatomite, (c,d) Platy shape of diatomite.

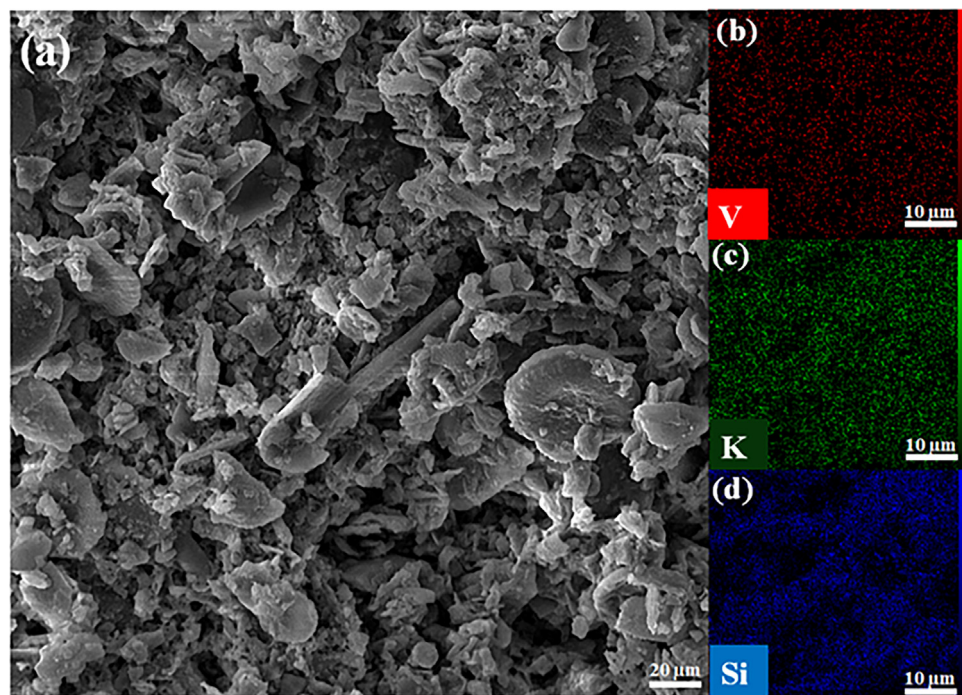


Fig. 10. (a) SEM image of VaCe0, (b) Elemental mapping images of vanadium (c) Potassium (d) Si.

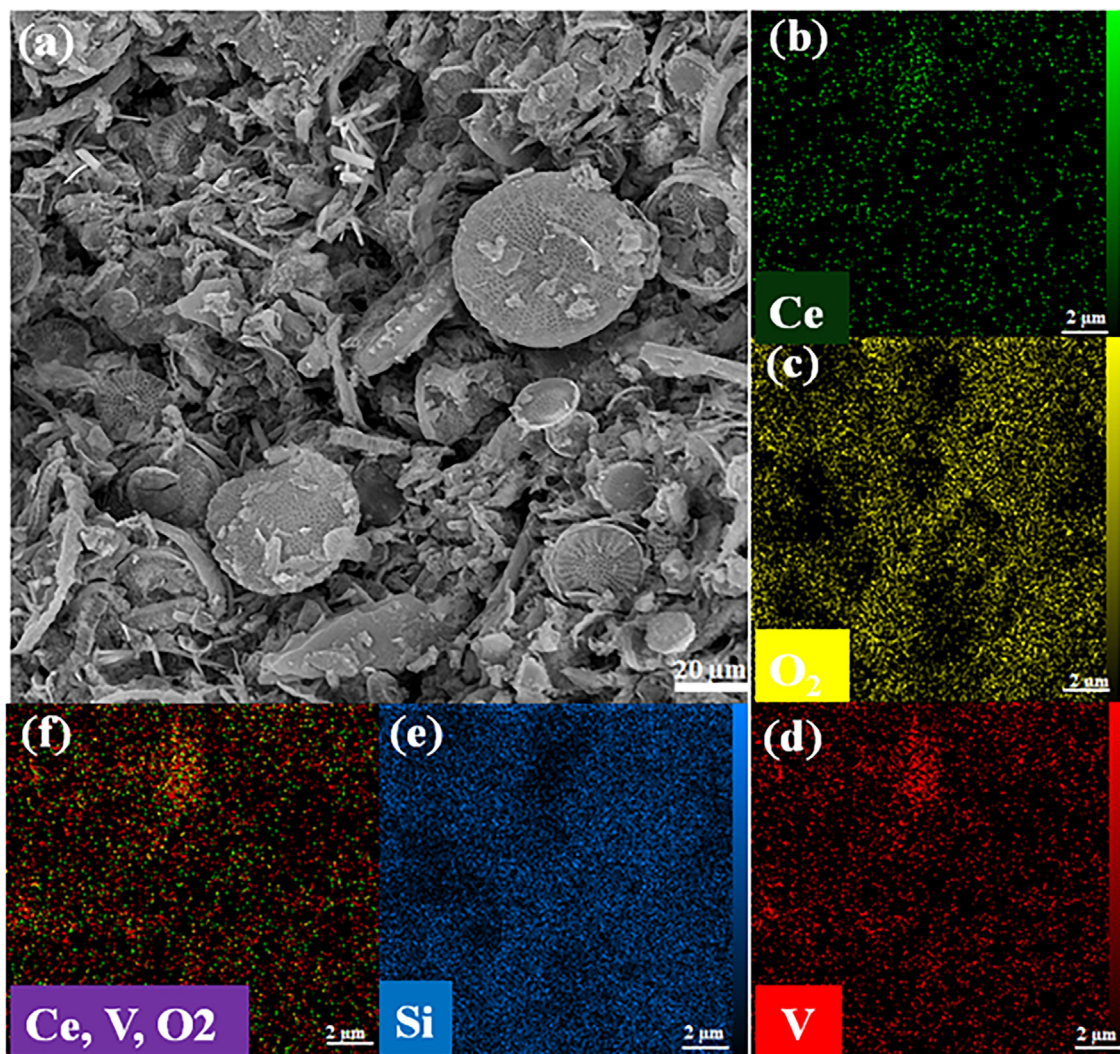


Fig. 11. (a) SEM analysis of VaCe7 sample, (b) Elemental mapping images of cerium, (c) O₂, (d) Vanadium, (e) Si and (f) Ce, V & O₂.

vanadium oxide (Code 01-083-1858) and diffraction peaks at 21.8, 38.6 and 44.6° for cristobalite low (code 01-076-0940).

Consequently, by adding ceria promoter to V₂O₅ catalyst, noteworthy changes were observed in VaCe7 pattern. Potassium cerium sulfate, cerium vanadium oxide and cerium oxide were seen in VaCe7 sample, which was related to Ce promoter. Cerium vanadium oxide (2CeVO₄ = Ce₂O₃ + V₂O₅) is the target component that can describe the role of Ce as a promoter in improving the kinetics of V₂O₅ (main catalytic component) in the SO₂ oxidation reaction. The heterogeneous catalytic reactions were performed on the surface of the catalyst, while XRD analysis showed the bulk properties of the catalyst. Hence, this result must be proved by XPS study to show the role of Ce on the surface of the catalyst, instead of the bulk.

3.5. SEM micrographs

SEM analysis and morphology of support (diatomaceous earth), which involved the skeleton of fossilized algae, can be seen in Fig. 9a–d. Unclogged pores of highly porous diatomite can be seen as the catalyst support with various shapes such as platy, cylindrical and acicular in these figures [63].

SEM images of VaCe0 and VaCe7 samples are shown in Figs. 10 and 11, respectively. Fig. 10 and 11 represent the coarse surface of the catalyst with irregular shapes. In order to study the

distribution of various elements on the catalyst, elemental mapping was used. Fig. 10 shows the surface of VaCe0 with the elemental mapping of V, K and Si. It can be seen that each of these elements was fully distributed on the surface of the catalyst. Fig. 11 displays the coarse surface of VaCe7 sample with elemental mappings of Ce, O₂, V and Si to study the dispersion of ceria promoter on the surface of the catalyst. It is observed that ceria promoter and vanadium had excellent distribution. XRD and FTIR tests showed the presence of CeVO₄ component in the catalyst. The elemental mapping of Fig. 11f confirmed the simultaneous existence of cerium, vanadium and oxygen, which might be related to CeVO₄. These results were in agreement with XRD and FTIR results.

SEM analysis of VaCe9 and VaCe11 can be observed in Fig. 12a and b. It can be demonstrated that with increasing ceria promoter from 7 to 11 wt.% on diatomite support, Ce had insufficient dispersion on the catalyst and can lead to the clog of the pores of the catalyst. This result was also in good agreement with the activity tests. The reduction in the pore sizes from VaCe0 to VaCe7 may be related to formation of higher amount of the crystal structure of CeVO₄. Accumulation of ceria promoter on the support of VaCe9 and 11 catalysts can be comprised by the observation of the diatomite support in Fig. 9, and VaCe9 and 11 catalysts in Fig. 12. Accumulation of ceria caused a decrease in the PSD of VaCe9 and 11 catalysts because of blocking the pores of diatomite. This result

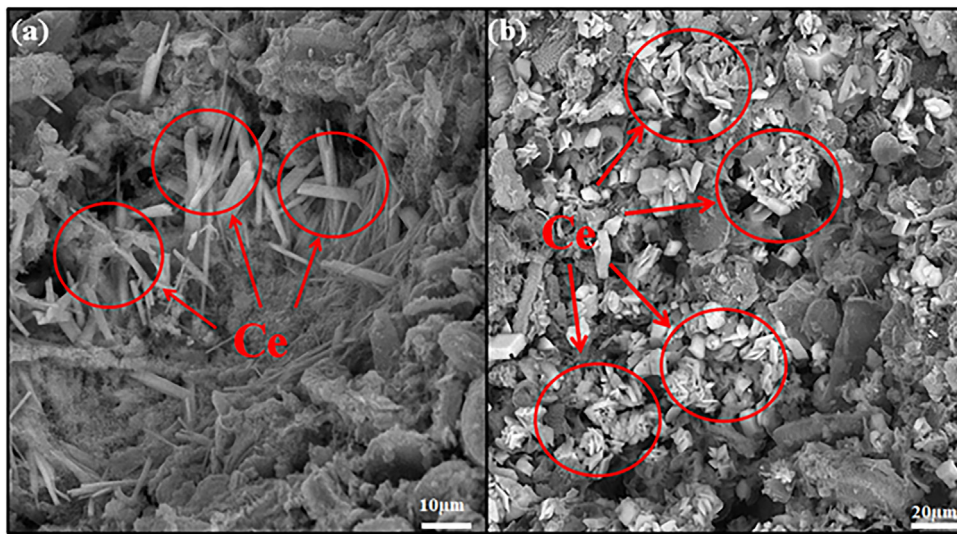


Fig. 12. Insufficient dispersion of cerium on V_2O_5 catalyst for (a) VaCe9 and (b) VaCe11.

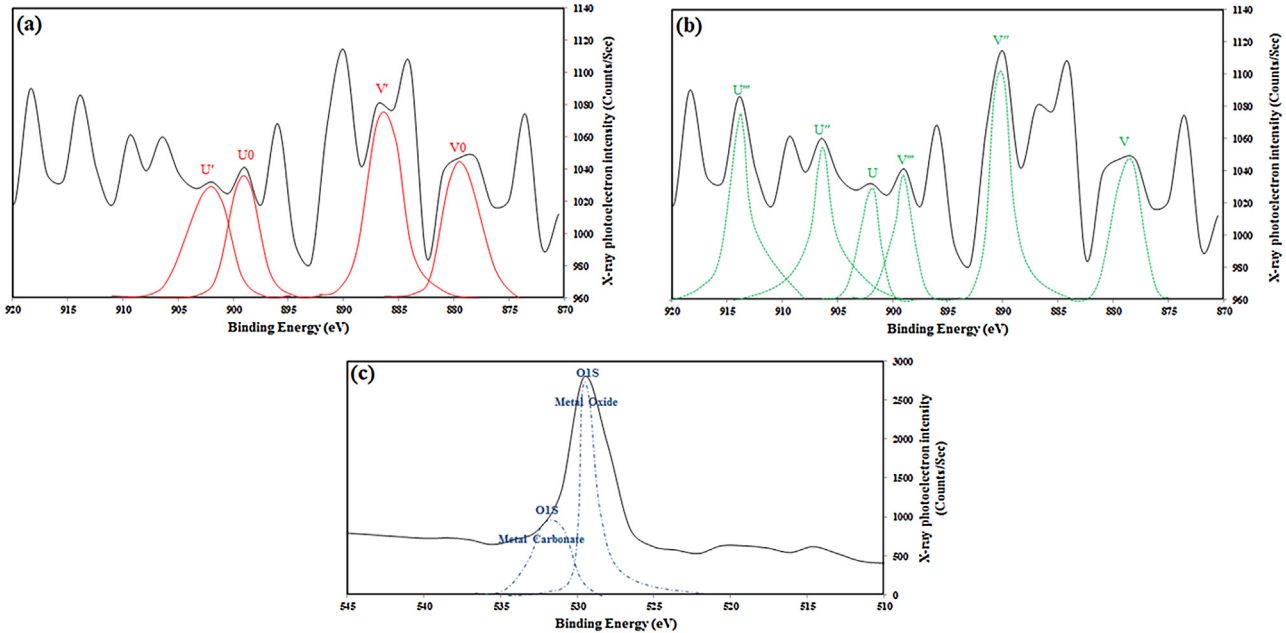


Fig. 13. (a) XPS spectra of Ce(III) (b) Ce(IV) and (c) O1S.

of SEM analysis was in agreement with the PSD results of VaCe9 and VaCe11.

3.6. XPS analysis

CeO_2 plays an outstanding role in oxidation reaction for two important factors: redox properties and high capacity of its lattice oxygen [64]. Deconvolution is used to evaluate cerium oxidation states. Fig. 13a shows the XPS spectra of Ce (III). There are two modes of orbitals such as $Ce\ 3d_{3/2}$ and $Ce\ 3d_{5/2}$. Peaks at higher energy u' and v' are located at binding energy of 903.4 eV, 887.1 eV, respectively. These peaks represent $Ce\ 3d^9\ 4f^1\ O2p^6$ final state and corresponded to $Ce\ 3d_{3/2}$ contribution. In addition, peaks at less energy u_0 and v_0 are located at 899 eV and 880 eV that are demonstrated $Ce\ 3d^9\ 4f^2\ O2p^5$ state and are corresponded to $Ce\ 3d_{5/2}$ contribution.

Fig. 13b presents the XPS spectra of CeO_2 (IV). In this component, different orbital modes such as $3d_{5/2}$ and $3d_{3/2}$ can be studied. Peaks

with the highest level of energy can be noted by u'' and v'' which can be seen at 916.4 eV and 893.3 eV, respectively. These peaks represented the orbital Ce valance of $3d^9\ 4f^{00}$ and oxygen valance of $O2p^6$. The peak at u'' demonstrated Ce(IV) with $Ce\ 3d_{3/2}$. Peaks with less energy can be noted as u , v , u'' and v'' by 901.8, 879, 909.1 and 890, respectively. The presence of CeO_2 in this XPS study was in good agreement with FTIR and XRD results.

Oxygen peaks showed a cerium oxidation state [65]. Fig. 13c demonstrates the spectra of O1S peaks at 529.8 eV and 531.5 for Ce(IV) and Ce(III), respectively. There was an energy difference (1.7 eV) between the two peaks of O1S.

There are various compounds of vanadium-oxygen that is important to study their different forms. Spectral lines of vanadium oxide satisfy the $V2p$ doublet [66]. The binding energy of $V2p$ should be raised when the oxidation state of vanadium is increased. In addition, the XPS peak fitting can be used for finding the lower oxidation state of vanadium (V^{4+} and lower) [67]. Fig. 14 shows the vanadium oxidation states that can be observed on the core

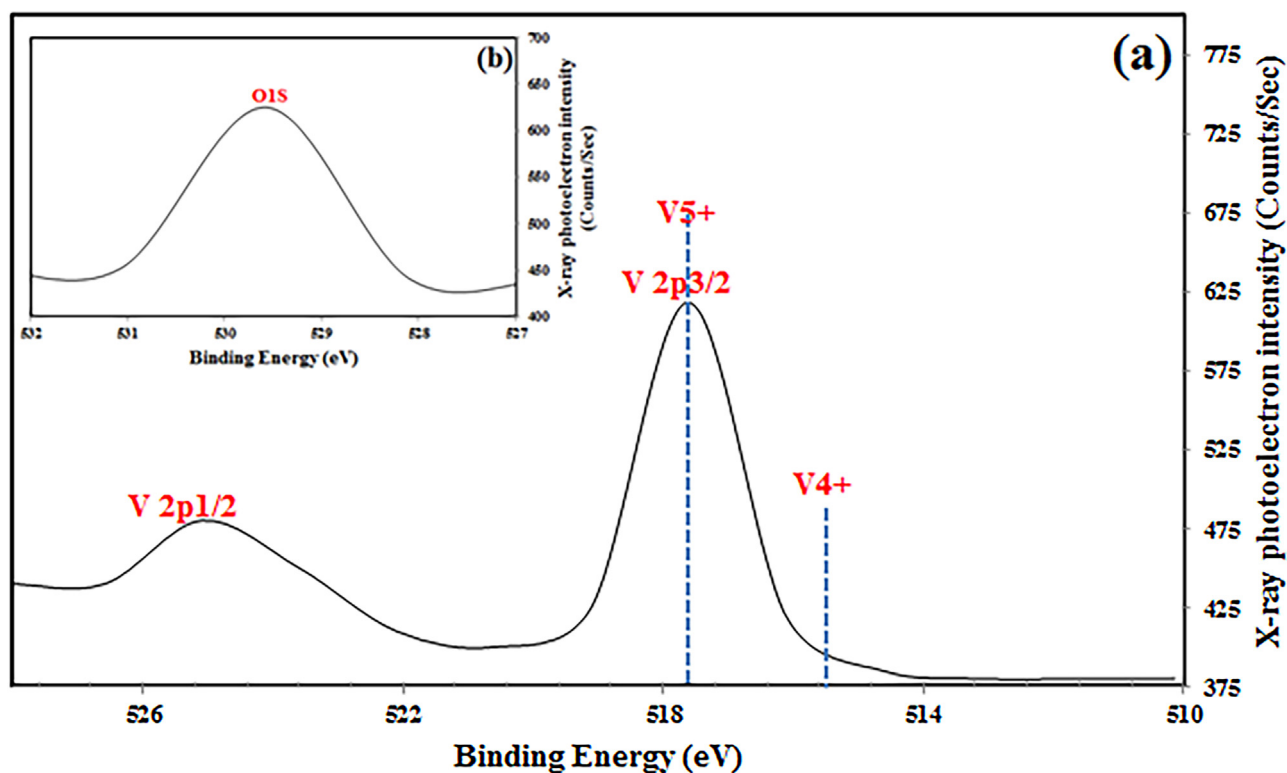


Fig. 14. XPS spectra of various vanadium cation oxidations (a) with the inset picture of O1S (b).

lines approximately at 516.0 and 517.7, corresponding to V⁴⁺ and V⁵⁺, respectively. The V⁵⁺ state of vanadium was abnormally higher than the ones mentioned in the literature [68–70]. Furthermore, the peaks can be seen at 529.9 eV for O1S displayed in the inset picture of Fig. 14. It may be concluded that CeO₂ is a linear molecule; however, Ce(III) can be a Ce₂O₃ molecule. Eventually, this molecule can be presented as hexagonal structure.

Information about the nature of ceria-vanadia interface species are not abundant [71,72]. Vanadium species on the surface of catalyst interact with ceria compounds and reduce Ce(IV) to Ce(III) and formation of CeVO₄ [73]. This phase of CeVO₄ was also observed in XRD and FTIR results of this article. Cerium and vanadium participated in the oxidation number of (III) and (V) in this component (CeVO₄), respectively. Free energy of the formation of Ce(III) was more than that of vanadium(V). Cerium with the atomic number of 58 had weaker effective nuclear charge than vanadium with the atomic number of 23. In addition, the electronegativity of vanadium and cerium was 1.63 and 1.12, respectively, which can cause stronger effective nuclear charge on the electron valance shell of vanadium than cerium. It may be concluded that cerium participated in oxidation and reduction reaction with less time and energy than vanadium. As a result, the energy barrier for the re-oxidation of CeO₂ was lower than V₂O₅ and these issues caused the need for less activation energy for the re-oxidation of CeO₂ than V₂O₅.

It can be concluded that Ce promoted V₂O₅ by the formation of CeVO₄ network, which reduced the activation energy of reduction-oxidation and increased the rate of the SO₂ oxidation reaction.

4. Conclusion

V₂O₅ catalyst promoted by ceria was studied in this work for the SO₂ oxidation reaction. Full factorial experimental design method including 315 experiments was applied to optimize the ceria promoter and study various interactions in the catalytic conversion. The results showed that ceria had a significant effect on catalyst

activity and the ceria loading of 7 wt.% led to reaching the maximum catalyst activity. Also, 135 post-experiments were performed based on another full factorial design to compare the catalyst with 7% ceria and without ceria at different levels of SO₂%, O₂/SO₂ ratio, temperature and GHSV. VaCe7 had higher mean conversion difference at less SO₂%, higher O₂/SO₂ ratio and less GHSV than VaCe0. VaCe7 always has more catalyst activity than VaCe0, showing that less mass of ceria promoted catalyst has the same activity as the higher amount of catalyst without ceria promoter in the convertor beds of the sulfuric acid plant. Therefore, using the less mass of VaCe7 reduces the bed pressure drop, which is a very important parameter in this plant. CeVO₄ was observed in XRD and FTIR results and was confirmed by XPS study. Cerium participated in oxidation and reduction reaction with less time and energy than vanadium. As a result, the energy barrier for the reduction-oxidation of CeO₂ was lower than V₂O₅. It can be concluded that ceria promoted V₂O₅ by the formation of CeVO₄ network, which reduces the activation energy of reduction-oxidation and increased the rate of the SO₂ oxidation reaction. The stability tests of VaCe0 and VaCe7 showed that both were stable during 50 h, but at the start-up, VaCe7 started by high conversion and reached a peak before being stable, which was not seen for VaCe0. This issue demonstrated that VaCe7 could reduce SO₂ emission at the start-up of the plant, which plays an important role for environmental protection. This preference can be described by the oxygen storage capacity of ceria that improves the rate of reaction by increasing the available oxygen for the reaction by oxygen transferring from ceria to vanadia.

References

- [1] D.K. Louie, *Handbook of Sulphuric Acid Manufacturing*, second ed., DKL Engineering, Inc, Richmond Hill, Ontario, Canada, 2008.
- [2] O.B. Lapina, B.S. Bal'zhinimaev, S. Boghosian, K.M. Eriksen, R. Fehrmann, *Catal. Today* 51 (1999) 469.
- [3] A. Urbanek, M. Treti, *Catal. Rev. – Sci. Eng.* 21 (1980) 73.

[4] B. Balzhinimaev, A. Ivanov, O. Lapina, V. Mastikhin, K. Zamarev, *Faraday Discuss. Chem. Soc.* 87 (1989) 133.

[5] O. Lapina, V. Mastikhin, A. Shubin, V. Krasilnikov, K. Zamaraev, *Prog. NMR Spectrosc.* 24 (1992) 457.

[6] C. Zhen-Xing, Y. Gang, Y. Hua, *Trans. Nonferrous Met. Soc. China* 11 (2001) 595.

[7] S.G. He, Y. Xie, F. Dong, S. Heinbuch, E. Jakubikova, J.J. Rocca, E.R. Bernstein, *J. Phys. Chem. A* 112 (2008) 11067.

[8] B.M. Reddy, A. Khan, Y. Yamada, T. Kobayashi, S. Loridan, J.C. Volta, *J. Phys. Chem. B* 107 (2003) 5162.

[9] J. Villandsen, H. Livbjerg, *Cat. Rev. – Sci. Eng.* 17 (1978) 203.

[10] A. Urbanek, M. Treti, *Catal. Rev. – Sci. Eng.* 21 (1) (1980) 73.

[11] S. Boghosian, R. Fehrmann, N.J. Bjerrum, G.N. Papatheodorou, *J. Catal.* 119 (1989) 121.

[12] B.S. Balzhinimaev, V.E. Ponomarev, G.K. Boreskov, A.A. Ivanov, V.S. Sheplev, E.M. Sadovskaya, *React. Kinet. Catal. Lett.* 28 (1985) 81.

[13] F.J. Doering, M.L. Unland, K.A. Berkel, *Chem. Eng. Sci.* 43 (1988) 221.

[14] B.S. Balzhinimaev, V.E. Ponomarev, N.P. Belyaeva, A.A. Ivanov, G.K. Boreskov, *React. Kinet. Catal. Lett.* 30 (1986) 23.

[15] C.K. Gupta, N. Krishnamurthy, In *Extractive Metallurgy of Rare Earths*, CRC Press, Boca Raton, 2004.

[16] S.L. Swartz, *J. Am. Chem. Soc.* 124 (2002) 12923.

[17] M.S. Moreno, F. Wang, M. Malac, T. Kasama, C.E. Gigola, I. Costilla, M.D. Sánchez, *J. Appl. Phys.* 105 (2009) 083531.

[18] M.A. Bañares, M.V. Martínez-Huerta, X. Gao, J.L.G. Fierro, I.E. Wachs, *Catal. Today* 2116 (2000) 1.

[19] M.A. Bañares, M.V. Martínez-Huerta, X. Gao, I.E. Wachs, J.L.G. Fierro, *Stud. Surf. Sci. Catal.* 130 (2000) 3125.

[20] T. Feng, J.M. Vohs, *J. Catal.* 221 (2004) 619.

[21] M.V. Martínez-Huerta, J.M. Coronado, M. Fernandez-Garcia, A. Iglesias-Juez, G. Deo, J.L.G. Fierro, M.A. Banares, *J. Catal.* 225 (2004) 240.

[22] H.C. Yao, Y.F. Yu Yao, *J. Catal.* 86 (1984) 254.

[23] S. Bedrane, C. Descorme, D. Duprez, *Catal. Today* 75 (2002) 401.

[24] C. Sun, H. Li, L. Chen, *Energy Environ. Sci.* 5 (2012) 8475.

[25] J. Li, G.Z. Lu, G.S. Wu, D.S. Mao, Y.Q. Wang, Y. Guo, *Catal. Sci. Technol.* 2 (2012) 1865.

[26] J.S. Lisboa, L.E. Terra, P.R.J. Silva, H. Saitovitch, F.B. Passos, *Fuel Process. Technol.* 92 (2011) 2075.

[27] H.Y. Li, H.F. Wang, X.Q. Gong, Y.L. Guo, Y. Guo, G.Z. Lu, P. Hu, *Phys. Rev. B* 79 (2009) 193401.

[28] H.F. Wang, Y.L. Guo, G.Z. Lu, P. Hu, *Angew. Chem. Int. Ed.* 48 (2009) 8289.

[29] N. Laosiripojana, W. Sutthisripok, S. Assabumrungrat, *Chem. Eng. J.* 112 (2005) 13.

[30] W. Deng, J. DeJesus, H. Saltsburg, M. Flytzani-Stephanopoulos, *Appl. Catal. A* 291 (2005) 126.

[31] M. Skoglundh, E. Fridell, *Top. Catal.* 28 (2004) 79.

[32] M. Skoglundh, A. Törncrona, P. Thormählen, E. Fridell, A. Drewsen, E. Jobson, *Stud. Surf. Sci. Catal.* 116 (1998) 113.

[33] R.J. Gorte, *AIChE J.* 56 (2010) 1126.

[34] N.V. Skorodumova, S.I. Simak, B.I. Lundqvist, I.A. Abrikosov, B. Johansson, *Phys. Rev. Lett.* 89 (2002) 166601.

[35] Y. Yang, C.O. Hernandez, P. Pizzaro, V.A. de la Pena Oshea, J.M. Coronado, D.P. Serrano, *Appl. Catal. B: Environ.* (2016), <http://dx.doi.org/10.1016/j.apcatb.2016.01.001>.

[36] A.N. Mendes, V.L. Zholobenko, F.T. Starzyk, P.D. Costa, C. Henriques, *Appl. Catal. B: Environ.* 195 (2016) 121.

[37] A.H. Pizarro, C.B. Molina, J.L.G. Fierro, J.J. Rodriguez, *Appl. Catal. B: Environ.* (2016), <http://dx.doi.org/10.1016/j.apcatb.2016.02.056>.

[38] F. Arena, B. Gumina, A.F. Lombardo, C. Espro, A. Patti, L. Spadaro, L. Spiccia, *Appl. Catal. B: Environ.* 162 (2015) 260.

[39] D. Taieb, A.B. Brahim, C.R. Chimie, C. R. Chim. 16 (2013) 39.

[40] P. Roy, A. Sardar, *J. Chem. Eng. Process Technol.* 6 (2015) 230.

[41] M. Mazidi, R.M., Behbahani, A. Fazeli, *Mater Res Innov.* (2016), (in press).

[42] J.L. Harris, J.R. Norman, *Ind. Eng. Chem. Process Des. Dev.* 11 (1972) 564.

[43] F. Meshkani, M. Rezaei, *Int. J. Hydrogen Energy* 39 (2014) 18302.

[44] N. Laosiripojana, W. Sutthisripok, S. Assabumrungrat, *Chem. Eng. J.* 112 (2005) 13.

[45] C.J. Zhang, A. Michaelides, S. Jenkins, *J. Phys. Chem. Chem. Phys.* 13 (2010) 22.

[46] F. Esch, S. Fabris, L. Zhou, T. Montini, C. Africh, P. Fornasiero, G. Comelli, R. Rosei, *Science* 309 (2005) 752.

[47] H.J. Kwon, J.H. Baik, Y.T. Kwon, I.-S. Nam, S.H. Oh, *Chem. Eng. Sci.* 62 (2007) 5042.

[48] D.C. Sayle, S.A. Maicaneanu, G.W. Watson, *J. Am. Chem. Soc.* 124 (2002) 11429.

[49] W. Liu, C. Wadia, M. Flytzani-Stephanopoulos, *Catal. Today* 28 (1996) 391.

[50] C.C. Chang, *J. Catal.* 53 (1978) 374.

[51] M. Bensitel, O. Saur, J.-C. Lavalley, G. Mabilon, *Mater. Chem. Phys.* 19 (1988) 147.

[52] A.M. Shor, A.A. Dubkov, A.I. Rubaylo, N.I. Pavlenko, O.M. Sharonova, A.G. Anshits, *J. Mol. Struct.* 267 (1992) 335.

[53] D.A. Bulushev, L. Kiwi-Minsker, F. Rainone, A. Renken, *J. Catal.* 205 (2002) 115.

[54] M. Kantscheva, I. Cayirtepe, A. Naydenov, G. Ivanov, *J. Catal. Today* 176 (2011) 437.

[55] A. Kato, K. Tomoda, I. Mochida, T. Seiyama, *Bull. Chem. Soc. Jpn.* 45 (1972) 690.

[56] S. Thakur, P. Patil, *Sens. Actuators B-Chem.* 194 (2014) 260.

[57] M. Ksibi, E. Elaloui, A. Houas, N. Moussa, *Appl. Surf. Sci.* 220 (2003) 105.

[58] J.M. Miller, L.J. Lakshmi, *J. Catal.* 184 (1999) 68.

[59] A.M. Duarte de Farias, P. Bargiela, M. da G.C. Rocha, M.A. Fraga, *J. Catal.* 260 (2008) 93.

[60] Y. Zheng, J. Jiang, Q. Yang, P. Tang, *Ap3er* (2015).

[61] X. Yang, W. Zuo, F. Li, T. Li, *Chemistryopen* 4 (2015) 288.

[62] M.L. Pang, J. Lin, M. Yu, S.B. Wang, *J. Solid State Chem.* 177 (2004) 2237.

[63] S.S. Ibrahim, A.Q. Selim, *Ore Dress. J.* 2 (2010) 25.

[64] A. Trovarelli, *Catal. Rev. – Sci. Eng.* 38 (1996) 439.

[65] E.J. Preisler, O.J. Marsh, R.A. Beach, T.C. McGill, *J. Vac. Sci. Technol. B* 19 (2001) 1611.

[66] G. Silversmit, D. Depla, H. Poelman, G.B. Marin, R. De, Gryse, *Surf. Sci.* 600 (2006) 3512.

[67] G. Silversmit, D. Depla, H. Poelman, G.B. Marin, R.D. Gryse, *J. Electron. Spectrosc. Relat. Phenom.* 135 (2004) 167.

[68] J. Mendialdua, R. Casanova, Y. Barbaux, *J. Electron. Spectrosc. Relat. Phenom.* 71 (1995) 249.

[69] G.A. Sawatzky, D. Post, *Phys. Rev. B* 20 (1979) 1546.

[70] M. Demeter, M. Neumann, W. Reichelt, *Surf. Sci.* 41 (2000) 454.

[71] M.A. Bañares, X. Gao, J.L.G. Fierro, I.E. Wachs, *Stud. Surf. Sci. Catal.* 110 (1997) 295.

[72] W. Daniell, A. Ponchel, S. Kuba, F. Anderle, T. Weingand, D.H. Gregory, H. Knözinger, *Top. Catal.* 20 (2002) 65.

[73] M.V. Martinez-huerta, J.M. Coronado, M. Fernandez-garcia, A. Iglesias-juez, G. Deo, J.L.G. Fierro, M.A. Banares, *J. Catal.* 225 (2004) 240.